Finite element analysis of shear capacity of GFRP perforated plate connectors

Zheng Xiao[a], Dongyan Xue[b*], Yao Li[c], Yiduo Zhang[d]

xz9804@126.com[a], dyxue2008@163.com[b*], ly15610181927@163.com[c], Zhangzyd0927@tom.com[d]

School of Civil Engineering and Architecture, Jiangsu University of Science and Technology, Zhenjiang 212100, China[1]

Abstract: The finite element model was established by ABAQUS software to simulate the push-out test of GFRP perforated plate connectors. The reliability of numerical simulation was verified by comparing with the test results. Then, using the strength grade of concrete and the strength of perforated rebar as the changing parameters, the influencing factors of the shear capacity of the GFRP perforated plate connectors are explored. The test results indicate that increasing the strength level of concrete, the strength of perforated rebar can improve the shear capacity of the GFRP perforated plate connectors.

Keywords: Push-out test, Perforated plate connectors, Finite element model, GFRP

1 INTRODUCTION

Glass fiber reinforced composite material is one of FRP materials, which refers to a resin matrix reinforced with glass fiber, has the advantages of light, strong and easy to transport. So, it has broad application prospects in bridges. GFRP perforated plate can increase the bending stiffness of the structure, reduce structural deformation, and have better corrosion resistance. For the past few years, they have attracted more and more attention from researchers. [4, 6, 9]

Zou et al. (2019) obtained the conclusion that the slip modulus increases with the thickness of the perforated plate through the push-out test of FRP perforated plate connectors, and established the calculation equation of the shear capacity and slip modulus of FRP perforated plates. Xue et al. (2014) conducted a trial research on the push-out specimens of FRP perforated plates under monotonic static load. The results indicate the failure mode of the FRP perforated plate connectors shear test is the shear failure of the FRP perforated plate root. Di et al. (2020) conducted a monotonic push-out test on GFRP perforated plate specimens, analyzed the influence of hole number and hole spacing on the performance of the perforated plate, and concluded that the shear capacity of the perforated plate decreases with the increase of the number of rows and gradually increases with the increase of spacing.

The paper uses ABAQUS finite element software to simulate the nonlinear finite element analysis of GFRP perforated plate connectors by simulating the push-out test, and studies the effects of different structural parameters on the shear capacity of GFRP perforated plate connectors.

EMIS 2023, February 24-26, Chengdu, People's Republic of China

DOI 10.4108/eai.24-2-2023.2330641

At present, there is relatively a little finite element research on the shear performance of GFRP perforated plate connectors. Compared with actual test, finite element analysis has the advantages of low cost, unlimited space and more accurate calculation results [4].

Therefore, the paper uses ABAQUS finite element software to simulate the nonlinear finite element analysis of GFRP perforated plate connectors by simulating the push-out test, and studies the effect of different structural parameters on the shear capacity of GFRP perforated plate connectors. Based on the existing experimental data, the simulated data are compared and analyzed to verify the reliability of the numerical simulation analysis and provide more reference for the design and application of GFRP perforated plate connectors.

2 TEST SPECIMENS AND PARAMETERS

Based on the research of Di et al., this paper designs the following sizes of the specimens, which are shown in Figure 1. The parameters studied include the concrete strength, the strength of perforated rebar. You can see the parameters of the specimens in Table 1.

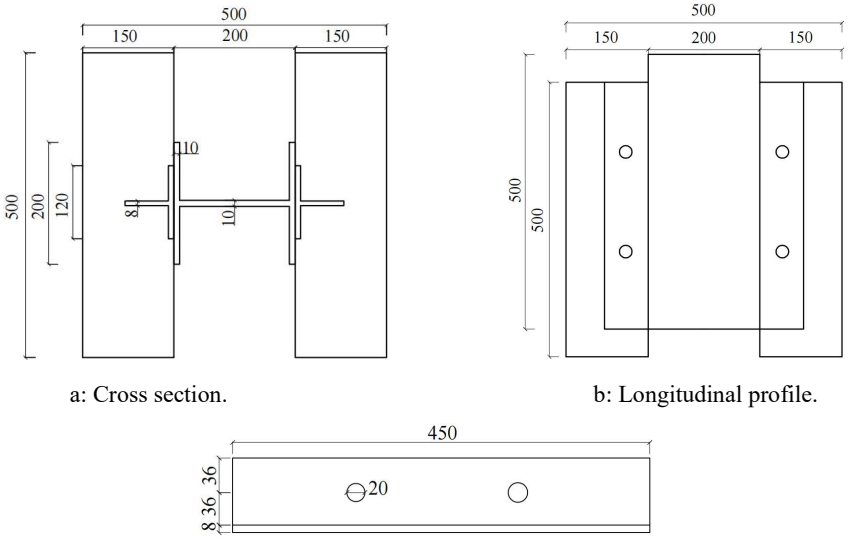

a: Cross section. b: Longitudinal profile.

c: Dimensions of perforated rib shear connectors.

Figure 1: Dimensions of specimen (Units: mm).

Table 1: Parameters of the specimens.

Specimens	Concrete strength/Mpa	The strength of perforated rebar/Mpa
PBL-1-1	50	400
PBL-1-2	40	400
PBL-1-3	30	400
PBL-2-1	50	335
PBL-2-2	50	400
PBL-2-3	50	500

3 ESTABLISHMENT OF FINITE ELEMENT MODEL

In the paper, a half of the simplified model of the actual test is established according to the symmetry of the structure, and the ABAQUS software is used.

3.1 Material constitutive relation model

The paper refers to the concrete constitutive model based on the research of Lubliner and Lee and Fenves in ABAQUS software (Pasca, 2014).

$$\sigma = \begin{cases} \varepsilon E_c & \left(\varepsilon \leq 0.4 f_c / E_c\right) \\ \left(\dfrac{kn - n^2}{1+(k-2)n}\right) f_c & \left(0.4 f_c / E_t \leq \varepsilon \leq \varepsilon_c\right) \\ f_c - \dfrac{f_c - 0.85 f_c}{\alpha\varepsilon_c - \varepsilon_c}(\varepsilon - \varepsilon_c) & \left(\varepsilon_c < \varepsilon < \alpha\varepsilon_c\right) \end{cases} \tag{1}$$

In the formulas, E_c refers to the elastic modulus of concrete, ε_c takes 0.0025, k refers to the plasticity index, E_c / f_c, α is 1.75 according to the linear interpolation method, n refers to $\varepsilon/\varepsilon_c$, f_c refers to the cube compressive strength of concrete.

$$f = \begin{cases} \varepsilon E_c & (\varepsilon \leq \varepsilon_t) \\ f_t - \dfrac{f_t}{(\beta - 1)\varepsilon_t}(\varepsilon - \varepsilon_t) & (\varepsilon \geq \varepsilon_t) \end{cases} \tag{2}$$

In the formula, f_t refers to the design value of tensile strength of concrete, ε_t refers to the cracking strain of concrete, β takes 50.

The steel bar adopts the bilinear constitutive relation [3], which is shown in Figure 4, and the calculation formula is equation (3).

$$\sigma = \begin{cases} \varepsilon E_s & \left(\varepsilon \leq \varepsilon_y\right) \\ \sigma_y & \left(\varepsilon \geq \varepsilon_y\right) \end{cases} \tag{3}$$

In the formula, σ_y is the yield strength of the rebar, ε_y is the corresponding yield strain when the steel bar reaches the yield strength, and E_s is the elastic modulus of the rebar.

Different from steel and concrete, GFRP profiles are anisotropic materials [7]. Therefore, it is necessary to consider the difference of elastic modulus, shear modulus and Poisson's ratio in all directions of GFRP materials in finite element simulation. In the simulation of this paper, it is assumed that the GFRP material is linear elastic in the three main directions, and the engineering constants are used to represent the properties of the three main directions. The corresponding formula [10] is shown in equation (4).

$$\sigma_f = \begin{cases} E_f \varepsilon_f & 0 \leq \varepsilon \leq \varepsilon_f \\ 0 & \varepsilon_f \geq \varepsilon_{fu} \end{cases} \tag{4}$$

In the formula, σ_f is the tensile stress of FRP, E_f is the elastic modulus in the direction of FRP fiber, ε_f is the tensile strain of FRP, and ε_{fu} is the ultimate tensile strain of FRP material.

3.2 Element type selection and meshing

In the push-out test of numerical simulation in this paper, concrete, concrete tenon, H-shaped GFRP plate, perforated rebar and GFRP perforated plate are all modeled by Solid. When dividing the grid of H-shaped GFRP plate and GFRP perforated plate, it is divided into two layers along their respective thickness directions to roughly simulate the stratification of GFRP profiles, and assume that the mechanical properties of the two layers are the same. The meshing of the model is shown in Figure 2.

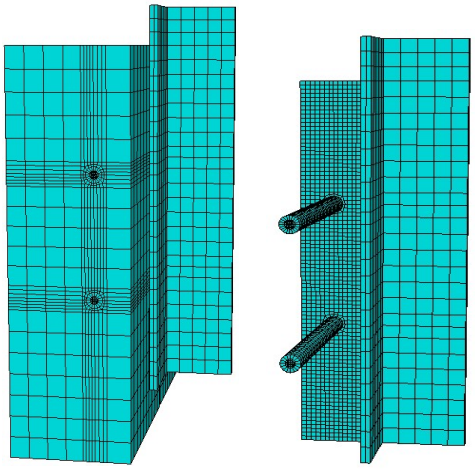

Figure 2: Finite element model.

3.3 Interaction

In the simulation of push-out test, there are five mutual contacts, among which the contact between rebar and concrete tenon, concrete tenon and concrete block, GFRP perforated plate and H-type GFRP plate is simulated by Tie constraint. The Contact is used between the perforated plate and the concrete tenon, the perforated plate and concrete block. The normal direction is adopted by hard contact, and the tangential direction is simulated by the friction property with a friction coefficient of 0.4.

3.4 Boundary conditions and loading

In the push-out test simulation, where the boundary condition of the bottom of the concrete block is completely fixed (U1=U2=U3=0), and the degree of freedom of all directions at the bottom of the concrete is constrained. The boundary condition of on the symmetrical section of H-shaped GFRP plate is that the bending moment in X and Z directions is zero, and the other directions are free (U2= UR1=UR3=0). A coupling constraint coupled to the centroid point is applied to the top of the H-shaped GFRP plate to avoid the influence of eccentric loading on the test results.

4 SIMULATION RESULTS AND ANALYSIS

4.1 Load-slip curve characteristics and verification

The corresponding load-displacement curve is shown in Figure 3. We can see from the figure that the shear process of GFRP perforated plate can be roughly divided into two stages: elastic stage and plastic stage. In the elastic stage, the trend of the test curve is consistent with the numerical simulation curve. The specimens begin to completely enter the plasticity at 2 mm, and the front stiffness is slightly smaller than the test, which is caused by the simplification of the model in the finite element simulation. In the plastic stage, with the gradual increase of relative displacement, the growth of load gradually decreases. At the same time, the test curve is in good agreement with the simulation curve, and the simulation method can be considered accurate.

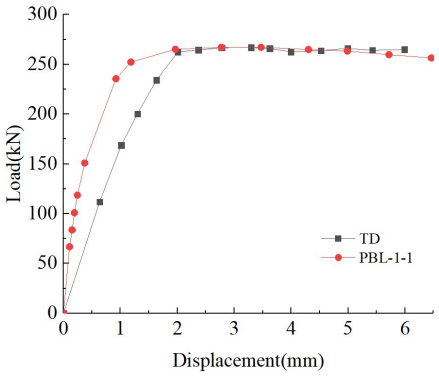

Figure 3: Comparison of finite element calculated values and experimental values.

4.2 Influence of concrete strength

When simulating the push-out test of GFRP perforated plate connectors, the specimens PBL-1-1, PBL-1-2 and PBL-1-3 correspond to the concrete strength grades of C50, C40 and C30 respectively, and other conditions are the same. The load-displacement curve got by simulation is shown in Figure 4.

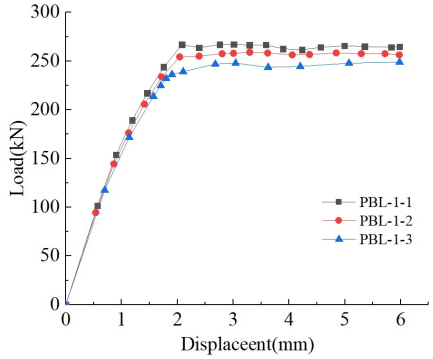

Figure 4: Effect of concrete strength on load-displacement curve.

As we can see, with the increase of concrete compressive strength, the shear capacity of GFRP perforated plate connector increases gradually. When the concrete strength grade increases from C30 to C40 and C50, the ultimate bearing capacity of GFRP perforated plate connector increases from 247.12kN to 257.54kN and 265.34kN.

4.3 Influence of the strength of perforated rebar

When simulating the push-out test of GFRP perforated plate connectors, the specimens PBL-2-1, PBL-2-2 and PBL-2-3 correspond to the strength of perforated rebar of 335MPa, 400MPa and 500MPa respectively, and other conditions are the same. Figure 5 shows that the load-displacement curve got by simulation.

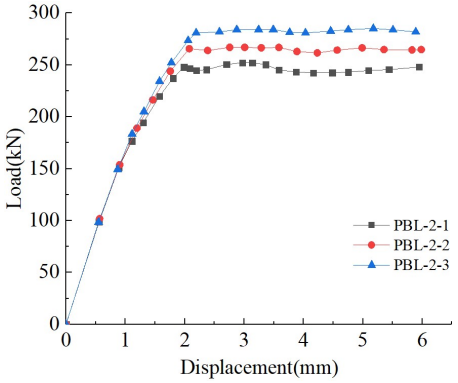

Figure 5: Effect of concrete strength on load -displacement curve.

From Figure 5, we can see that the shear capacity of GFRP perforated plate connectors will increase with the increase of the strength of perforated rebar. When the strength of the perforated rebar increases from 335MPa to 400MPa and 500MPa, the ultimate capacity of the GFRP perforated plate connectors increases from 251.80kN to 265.34kN and 284.52kN.

5 CONCLUSIONS

Through above finite element analysis of the shear capacity of GFRP perforated plate connectors, we can draw the following conclusion:

1) The higher the strength grade of concrete, the stronger the shear capacity of GFRP perforated plates connectors is.

2) The higher the strength of perforated rebar, the stronger the shear capacity of GFRP perforated plate connectors.

References

[1] Alexandre, P. (2020). European Committee for Standardization. Dictionary Geotechnical Engineering /wrterbuch Geotechnik. 486-486.

[2] Di J, Cao L, Han J. (2020). Experimental study on the shear behavior of GFRP-Concrete composite beam connections. J. Materials. 13(5): 1067.
[3] Huang Yangcheng, Xue Dongyan, Zhang Yiduo. (2021). Finite element analysis of shear capacity of T-shaped flange perfobond connector, J. Journal of Jiangsu University of Science and Technology (Natural Science Edition)，2,2021,35(06):100-106.
[4] Liu Jiaxin. (2020). Study on shear performance of GFRP-concrete composite structure with perforated plate connection. D. Hubei University of Technology.
[5] Xue Weichen, ZHANG Sai, GE Chang. (2014). Experimental study on shear connectors of FRP concrete composite beams. J. Journal of Highway and Transportation Research and Development. (1): 4.
[6] Nam, J H. (2007). Perforated FRP shear connectors for the FRP-Concrete composite bridge deck. J. Key Engineering Materials. 334-335(Pt1):381-384.
[7] Miao Lulu, Qu Qingshan. (2023). Mechanical properties of glass fiber reinforced composite steel composite truss beam. Ordnance Material Science and Engineering. 2023, 46(01): 68-73.
[8] Zou X X, Feng P, Wang J Q. (2016). Perforated FRP ribs Perforated FRP ribs for shear connecting of FRP-concrete hybrid beams decks. J. Composite Structures. 152 (sep.): 267-276.
[9] Zuo Y. et al. (2018). Flexural performance of a hybrid gfrp-concrete bridge deck with composite t-shaped perforated rib connectors. J. Composite Structures. 194: 263-278.
[10] Zheng Huakai. (2018).Simulation and fatigue experiment of GFRP-Concrete composite deck. D. Southeast University.
[11] Zuo Yize. et al. (2019). Experimental study on shear behavior of perforated GFRP shear connectors. Proceedings of 2019 Annual Academic Conference of Chinese Society of Civil Engineering. 560-569.